NUCLEAR SCIENCE AND TECHNIQUES **26**, 060602 (2015)

Speciation study of chromium corrosion product in molten LiF-NaF-KF salt*

QIU Jie (邱杰),[1,2] ZOU Yang (邹杨),[1] YU Guo-Jun (俞国军),[1] HE Shang-Ming (何上明),[1]
LIU Wen-Guan (刘文冠),[1] JIA Yan-Yan (贾彦彦),[1] LI Zhi-Jun (李志军),[1] and XU Hong-Jie (徐洪杰)[1,†]

[1]*Shanghai Institute of Applied Physics, Chinese Academy of Sciences, Shanghai 201800, China*
[2]*University of Chinese Academy of Sciences, Beijing 100049, China*

(Received January 28, 2015; accepted in revised form July 1, 2015; published online December 20, 2015)

To investigate the corrosion products of Cr in molten FLiNaK salt (46.5 mol% LiF–11.5 mol% NaF–42 mol% KF), the corrosion test of the pure metal Cr was performed in molten FLiNaK salt at 700 °C for 200 h. The FLiNaK salt after the corrosion test was thoroughly investigated by X-ray absorption near-edge structure spectroscopy, a transmission electron microscope, and X-ray diffraction. The results demonstrate that the predominant oxidation state of Cr in FLiNaK salt is Cr^{3+}, and the main corrosion product in cooled FLiNaK salt is K_2NaCrF_6.

Keywords: FLiNaK, Cr, Corrosion product, K_2NaCrF_6

DOI: 10.13538/j.1001-8042/nst.26.060602

I. INTRODUCTION

Among the reactor systems proposed in the Generation-IV International Forum, the molten salt reactor (MSR) has attracted much more attention due to its unique features, such as high thermodynamic efficiency, intrinsic safety, online refueling, etc. [1–4]. In the MSR, molten salt mixtures are used as the primary coolant or even as the fuel itself. These salts are characterized by high volumetric heat capacities, low viscosities, high boiling points, and other desirable features [5]. However, the molten salts are highly corrosive, especially at high temperatures. Corrosion of the structural materials in molten salt environments is one of the main challenges that prevent the MSR from long term operation [1]. A lot of work has been done in recent years to investigate the corrosion mechanisms of materials in molten salt environments [6–13]. It has been observed that among all the candidate structure materials for the MSR, the Cr composition was selectively attacked by molten fluoride salts and the corrosion rates were correlated with the Cr content of the alloys [6, 7].

In spite of the known tendency for Cr to be selectively attacked by molten fluoride salts, Cr is still widely used in high temperature alloys because it can improve the high-temperature oxidation resistance of the materials. Pure eutectic FLiNaK salt is emerging as a leading candidate salt for use as a secondary coolant for the MSR due to its advantageous thermal and physical properties [5, 14]. Therefore, a systematic study on the corrosion mechanism of Cr in molten FLiNaK salt is needed to ensure its safe application in MSR. To do this, one needs to understand the corrosion product of Cr in molten FLiNaK salts. However, to our knowledge, most of the research considers the case of the corrosion products of Cr in fluoride fuel salts and/or nitrates [14–16], in which uranium is the key factor in the corrosion process. A good understanding of fuel salt corrosion has been developed, but few data are available for pure coolant salts (e.g. FLiNaK). Therefore, the precise corrosion products of Cr in pure FLiNaK salt are highly desirable. Since the Cr content of most high temperature alloys is no more than 25wt.%, in order to yield sufficient concentrations of the corrosion products for identification, pure metal Cr was chosen for this research. In this work, metal Cr was exposed to molten FLiNaK salt in a graphite crucible at 700 °C for 200 h. After the corrosion test, the FLiNaK salt was investigated using X-ray absorption near-edge structure spectroscopy (XANES), a transmission electron microscope (TEM), and X-ray diffraction (XRD). The results show that the main corrosion product of Cr in FLiNaK salt is K_2NaCrF_6.

II. EXPERIMENT

The pure FLiNaK eutectic salt was supplied by Shanghai Institute of Organic Chemistry, Chinese Academy of Sciences. The impurities of the salt, detected by a Inductively Coupled Plasma-Optical Emission Spectrometer (ICP-OES), were as follows: 6 ppm Fe, 74 ppm Ni, 1 ppm Cr, 11 ppm Ca, 17 ppm Mg, 8 ppm Zn, and 6 ppm P. The content of H_2O was less than 100 ppm as determined using Carl-Fisher water analyzer. The high purity Cr was purchased from Beijing Cuibolin Non-ferrous Technology Developing Co., Ltd. The metal Cr used in this work are irregular metal pieces and the purity is 99.99%.

The corrosion test was performed in a graphite crucible due to the relative inertness of graphite to molten fluoride salts [6, 17]. A graphite crucible was made from purified graphite (CDI-1A). Prior to the corrosion test, the graphite crucible was ultrasonically cleaned in ethanol, and then baked at 800 °C for 12 h in a vacuum condition to expel contaminants, residual oxygen, and water. After the heat treatment,

* Supported by Science and Technology Commission of Shanghai Municipality (No. 11JC1414900), National Basic Research Program of China (No. 2010CB934501), the "Strategic Priority Research Program" of Chinese Academy of Sciences (No. XDA02040000), National Natural Science Foundation of China (Nos. 11005148 and 51371188), and the Special Presidential Foundation of Chinese Academy of Sciences, China (No. 29)

† Corresponding author, xuhongjie@sinap.ac.cn

the crucible was removed from the furnace and immediately stored in an argon atmosphere glove box. After that, 30 g of pure metal Cr pieces and 120 g of FLiNaK salt were placed in the graphite crucible. To ensure salt purity, the graphite crucible was sealed in a 316 stainless steel capsule and welded shut in the argon atmosphere glove box. The schematic diagram of the corrosion test capsule is shown in Fig. 1.

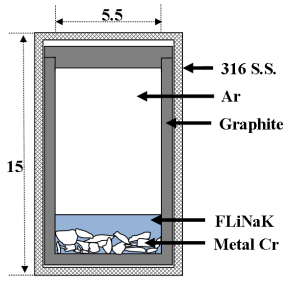

Fig. 1. (Color online) Schematic diagram of the capsule for the corrosion test at 700 °C for 200 h. Dimensions are in centimeters.

After the final weld, the capsule was transferred to a furnace and heated at 700 °C for 200 h. After the corrosion test, the capsule was cooled to room temperature and sliced open on the lathe. The Cr concentration of the FLiNaK salt after the corrosion test was analyzed by ICP-OES. The corrosion products were identified by XANES, TEM (FEI Tecnai G2 F20, 200 kV), and XRD (Rigaku D/max2500 V, Cu K_α, $\lambda = 0.154$ nm). The sample for the TEM was ultrasonically dispersed in ethanol and transferred to carbon-coated copper TEM grid. The Cr K-edge XANES spectra in the fluorescence yield mode were measured at the BL14W1 beamline of Shanghai Synchrotron Radiation Facility (SSRF) [18] which operates at an energy of up to 3.5 GeV and a stored current of 240 mA. The energy scale of the XANES spectra for the Cr K-edge (5.989 keV) was calibrated by a Cr metal foil. To avoid the impact of oxygen on the retrieved FLiNaK salt, all the salt samples were sealed in plastic bags during the XANES and XRD analysis processes.

III. RESULTS AND DISCUSSION

The cooled FLiNaK salt was retrieved after the corrosion test at 700 °C for 200 h. As shown in Fig. 2, the color of the FLiNaK salt changed from white to black-green after the corrosion test, which was mainly caused by the dissolution of Cr [19]. According to the results of ICP-OES analysis, the Cr and Ni contents of the FLiNaK salt after the corrosion test were (2403 ± 190) ppm and (4.4 ± 0.2) ppm, respectively. The concentration of Fe was below the quantitative detection limits of ICP-OES, as shown in Table 1. The Ni and Fe contents of the salt after the corrosion test were lower than that in the as-received salt. The main reason for this phenomenon is that Ni and Fe ions, which were introduced during the FLiNaK purification process, are consumed in the corrosion test via the following reaction [14, 19],

$$Ni^{2+} + Cr = Cr^{2+} + Ni(\Delta G_{700\,^\circ C} < 0), \quad (1)$$

$$Fe^{2+} + Cr = Cr^{2+} + Fe(\Delta G_{700\,^\circ C} < 0). \quad (2)$$

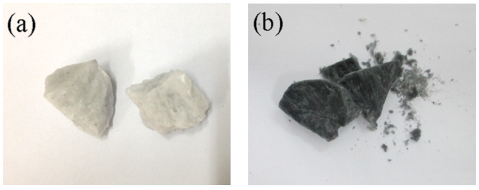

Fig. 2. (Color online) The FLiNaK salt (a) before and (b) after the corrosion test at 700 °C for 200 h.

TABLE 1. The analysis results of the salts before and after 700 °C, 200 h corrosion tests as examined by ICP-OES. All salts were tested in triplicate

FLiNaK salt	Cr content (ppm)	Ni content (ppm)	Fe content (ppm)
Before experiment	2.8	74	6
After experiment	2043 ± 190	4.4 ± 0.2	/

The reaction products Fe and Ni deposited on the surface of the metal Cr. Additionally, since it is a static corrosion test, the Cr corrosion product in the FLiNaK salt is not distributed evenly, especially at the contact area between the FLiNaK salt and the metal Cr. The Cr concentration of the salt is higher in the zone near the metal Cr. There are some green products at the salt-Cr interface.

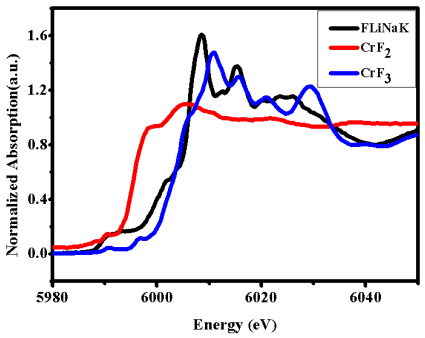

Fig. 3. (Color online) Normalized Cr K-edge XANES spectra of the post-experiment FLiNaK salt, CrF_2 and CrF_3.

Since XANES spectroscopy is sensitive to change in the Cr coordination environment, it was employed to determine the true oxidation state of Cr in FLiNaK salt after the corrosion test. Figure 3 shows the Cr K-edge XANES spectra of the post-experiment FLiNaK salt and the reference compounds (CrF_3, 99.98%, and CrF_2, 99%). Absorption edge shifts to a higher energy as the oxidation state of the material increases [20]. According to the edge position of the XANES spectra, it is clear that the edge position of the post-experiment FLiNaK salt, positioned at 6005 eV, agrees well with that in CrF_3. This indicates that the main oxidation state of Cr in FLiNaK salt is Cr^{3+}. It is known that FLiNaK salt

is a strong Lewis basic solvent, Cr^{2+} is not stable in molten FLiNaK salt [6, 21]. In the FLiNaK salt environment, the low oxidation ion Cr^{2+} would disproportionate in the following way [21, 22],

$$3Cr^{2+} = 2Cr^{3+} + Cr. \quad (3)$$

The alkali metal fluorides, i.e. FLiNaK salt, are ionic compounds, and the molten salt can easily give up their F^-. In molten FLiNaK salt, the Cr^{3+} ion would interact with F^- to form complexes, which will decrease the thermodynamic activity and stabilize the Cr^{3+} [6, 14, 22].

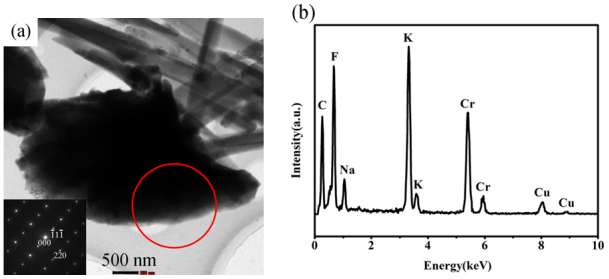

Fig. 4. (Color online) (a) TEM image of the post-experiment FLiNaK salt and (inset) SAED patterns of the red circle area, (b) EDS spectrum of the red circle area in (a).

The morphology and crystal structure of the post-experiment FLiNaK salt are characterized by the TEM. As depicted in Fig. 4(a), some black, irregular solid particles and rod-like crystals can be clearly observed in the typical TEM image. According to the EDS analysis, the rod-like crystals in the image correspond to the FLiNaK salt, whereas the black irregular particles contain Cr. Figure 4(b) presents the EDS spectrum of the black particle, only the peak of the elements F, Na, K, Cr, C, and Cu are shown in the spectrum. Since C and Cu contributed from the carbon-coated copper TEM grid, the EDS results indicate that the black particles are rich in F, Na, K, and Cr, which correspond to the Cr corrosion products. In order to determine the structure, the Cr-rich particles (black, irregular particles) are characterized by the selected area electron diffraction (SAED), as shown in Fig. 4(a). The lattice distances calculated from the diffraction dots are 4.76 Å (111), 2.88 Å (220), 2.45 Å (311), 2.40 Å (222), 1.83 Å (420), and 1.44 Å (440), which can be indexed to the standard face centered cubic K_2NaCrF_6 structure (Table 2). Silicon single crystals with a crystalline plane of (100) are used for calibration. Combined with the EDS results, it is confirmed that the Cr-rich black particle in the FLiNaK salt is K_2NaCrF_6. The lattice constant was calculated to be 8.21 Å, which correspond closely to the standard lattice constant of K_2NaCrF_6 (a=8.27 Å, space group symmetry *Fm3m*, JCPDS No.: 73-0415).

To further confirm the state of the Cr corrosion product, XRD was used to determine the structure of the salt after the corrosion test. Due to the low concentration of Cr in the post-experiment salt, the Cr corrosion products are hardly detected by XRD. Fortunately, some green product precipitates

TABLE 2. Comparison of d-spacing (in Å) from the present study and from the database

h k l	2θ (^{o})	*d*-spacing, SAED pattern (Å)	*d*-spacing, XRD (Å)	K_2NaCrF_6 standard *d*-spacing, (Å) (JCPDS:73-0415)
1 1 1	18.577	4.76	4.78	4.77
2 0 0	21.483		4.15	4.13
2 2 0	30.565	2.88	2.93	2.92
3 1 1	36.007	2.45	2.49	2.49
2 2 2	37.667	2.40	2.39	2.39
4 0 0	43.771		2.07	2.07
3 3 1	47.933			1.90
4 2 0	49.260	1.83		1.85
4 2 2	54.327		1.69	1.69
5 1 1	57.923		1.59	1.59
4 4 0	63.627	1.44	1.46	1.46
5 3 1	66.914		1.40	1.40
4 4 2	67.992			1.38
6 2 0	72.226		1.31	1.31

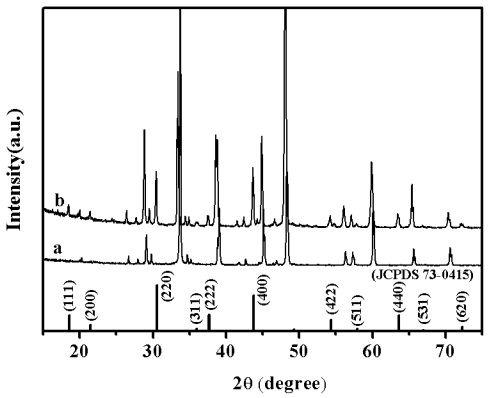

Fig. 5. XRD patterns of the FLiNaK salt (a) before and (b) after the corrosion test at 700 °C for 200 h. Bottom: standard XRD pattern of K_2NaCrF_6 (JCPDS No.: 73-0415).

out at the salt-Cr interface. The post-experiment salt containing the green product was characterized by XRD, as shown in Fig. 5. Compared to the XRD patterns of pure FLiNaK salt, some new diffraction peaks appear on the post-experimental FLiNaK salt. Although the new peaks are wide and weak because of the low concentration of the corrosion product, the new diffraction peak positions correspond closely to the diffraction peaks of K_2NaCrF_6. The calculated d-spacing values and the corresponding Miller indexes are given in Table 2. These values match well with the standard diffraction patterns of K_2NaCrF_6. The new peaks can be indexed to the face-centered cubic structure K_2NaCrF_6 (JCPDS No.: 73-0415). Comparing Fig. 5(a) with Fig. 5(b), it can be found that the diffraction peaks of the FLiNaK salt after the corrosion test are smaller than their corresponding counterparts of the salt before the corrosion test. According to the Bragg equation, this indicates that the interlayer distance of the salt increased after the corrosion test. As is known, the Cr atomic radius is larger than that of K and Na, the lattice parameters of the FLiNaK salt slightly increase when Cr dissolves into the salt.

The XRD results are in good agreement with that obtained from SAED and EDS analysis, which further verified that the corrosion product of Cr in FLiNaK salt is K_2NaCrF_6.

As mentioned above, the corrosion product of Cr in cooled FLiNaK salt is confirmed to be K_2NaCrF_6. The corrosion reaction in molten FLiNaK salt can be expected to reasonably satisfy the following equation:

$$CrF_3 + 2KF + NaF = K_2NaCrF_6. \quad (4)$$

In addition, the FLiNaK salt used as the reactor coolant is working under a high temperature molten state, therefore, future studies will consider whether the structure of Cr in high temperature molten FLiNaK salt is consistent with that in cooled FLiNaK salt.

IV. CONCLUSION

In summary, pure metal Cr was exposed to molten FLiNaK salt in a graphite crucible at 700 °C for 200 h. Due to the dissolution of Cr, it was found that the color of the FLiNaK salt changed from white to black-green after the corrosion test. XANES spectra revealed that the predominant oxidation state of Cr in FLiNaK salt is Cr^{3+}. The detailed structural characterizations confirm that the main corrosion product of Cr in cooled FLiNaK salt is K_2NaCrF_6. Based on the indexing in the SAED and XRD patterns, the Cr corrosion product appears to be a face centered cubic structure with a lattice constant of $a \approx 8.21$ Å.

[1] Rosenthal M, Haubenreich P and Briggs R. The development status of molten-salt breeder reactors. ORNL-4812. Oak Ridge, Tennessee, USA, 1972.

[2] Rosenthal M, Kasten P and Briggs R. Molten salt reactors–history, status, and potential. Nucl Appl Technol, 1970, **8**: 107–117.

[3] Serp J, Allibert M, Beneš O, *et al*. The molten salt reactor (MSR) in generation IV: Overview and perspectives. Prog Nucl Energy, 2014, **77**: 308–319. DOI: 10.1016/j.pnucene.2014.02.014

[4] Cai J, Xia X B, Chen K, *et al*. Analysis on reactivity initiated transient from control rod failure events of a molten salt reactor. Nucl Sci Tech, 2014, **25**: 030602. DOI: 10.13538/j.1001-8042/nst.25.030602

[5] Williams D F. Assessment of candidate molten salt coolants for the NGNP/NHI Heat-Transfer Loop, in: ORNL/TM-2006/69. Oak Ridge, Tennessee, USA, 2006.

[6] Olson L C, Ambrosek J W, Sridharan K, *et al*. Materials corrosion in molten LiF-NaF-KF salt. J Fluorine Chem, 2009, **130**: 67–73. DOI: 10.1016/j.jfluchem.2008.05.008

[7] Ouyang F Y, Chang C H, You B C, *et al*. Effect of moisture on corrosion of Ni-based alloys in molten alkali fluoride FLiNaK salt environments. J Nucl Mater, 2013, **437**: 201–207. DOI: 10.1016/j.jnucmat.2013.02.021

[8] Ouyang F Y, Chang C H and Kai J J. Long-term corrosion behaviors of Hastelloy-N and Hastelloy-B3 in moisture-containing molten FLiNaK salt environments. J Nucl Mater, 2014, **446**: 81–89. DOI: 10.1016/j.jnucmat.2013.11.045

[9] Kondo M, Nagasaka T, Tsisar V, *et al*. Corrosion of reduced activation ferritic martensitic steel JLF-1 in purified Flinak at static and flowing conditions. Fusion Eng Des, 2010, **85**: 1430–1436. DOI: 10.1016/j.fusengdes.2010.03.064

[10] Kondo M, Nagasaka T, Xu Q, *et al*. Corrosion characteristics of reduced activation ferritic steel, JLF-1 (8.92Cr-2W) in molten salts Flibe and Flinak. Fusion Eng Des, 2009, **84**: 1081–1085. DOI: 10.1016/j.fusengdes.2009.02.046

[11] Liu M, Zheng J, Lu Y, *et al*. Investigation on corrosion behavior of Ni-based alloys in molten fluoride salt using synchrotron radiation techniques. J Nucl Mater, 2013, **440**: 124–128. DOI: 10.1016/j.jnucmat.2013.04.056

[12] Sellers R S, Cheng W J, Kelleher B C, *et al*. Corrosion of 316L Steel Alloy and Hastelloy-N Superalloy in molten Eutectic LiF-NaF-KF Salt and interaction with Graphite. Nucl Technol, 2014, **188**: 192–199. DOI: 10.13182/NT13-95

[13] Qiu J, Zou Y, Yu G, *et al*. Compatibility of container materials with Cr in molten FLiNaK salt. J Fluorine Chem, 2014, **168**: 69–74. DOI: 10.1016/j.jfluchem.2014.09.010

[14] Williams D F, Toth L M and Clarno K T. Assessment of candidate molten salt coolants for the advanced high temperature reactor (AHTR), in: ORNL/TM-2006/12. Oak Ridge, Tennessee, USA, 2006.

[15] Koger J W. Corrosion and mass transfer characteristics of $NaBF_4$–NaF (92mol%–8mol%) in Hastelloy N. Oak Ridge National Laboratory, ORNL-TM-3866. Oak Ridge, Tennessee, USA, 1972.

[16] Briant R C, Buck J H and Miller A J, Aircraft nuclear propulsion project quarterly progress report. Oak Ridge National Laboratory, ORNL-1294. Oak Ridge, Tennessee, USA, 1952.

[17] Grimes W R. Molten-salt reactor chemistry. Nucl Technol, 1970, **8**: 137–155.

[18] Yu H S, Wei X J, Li J, *et al*. The XAFS beamline of SSRF. Nucl Sci Tech, 2015,**5**: 050102. DOI: 10.13538/j.1001-8042/nst.26.050102

[19] Olson L C. Materials corrosion in molten LiF-NaF-KF eutectic salt. Ph.D. Thesis, University of Wisconsin-Madison, 2009.

[20] Wong J, Lytle F, Messmer R, *et al*. K-edge absorption spectra of selected vanadium compounds. Phys Rev B, 1984, **30**: 5596–5610. DOI: 10.1103/PhysRevB.30.5596

[21] Jordan W H, Cromer S J, Strough R I, *et al*. Aircraft nuclear propulsion project quarterly progress report. Oak Ridge National Laboratory, ORNL-1896. Oak Ridge, Tennessee, USA, 1955.

[22] Sohal M S, Ebner M A, Sabharwall P, *et al*. Engineering database of liquid salt thermophysical and thermochemical properties. Idaho National Laboratory, INL/EXT-10-18297. Idaho Falls, Idaho, USA, 2010.